# Influence of Cyclic Dimer Formation on the Phase Behavior of Carboxylic Acids

Jiri Janecek and Patrice Paricaud*

Unité d'enseignement et de recherche de Chimie et Procédés (UCP), École Nationale Supérieure de Techniques Avancées (ENSTA), 75739 Paris, cedex 15, France

ABSTRACT: A new thermodynamic approach based on the Sear and Jackson association theory for doubly bonded dimers [*Mol. Phys.* 1994, 82, 1033] is proposed to describe the thermodynamic properties of carboxylic acids. The new model is able to simultaneously represent the vapor pressures, saturated densities, and vaporization enthalpies of the shortest acids and is in a much better agreement with experimental data than other approaches that do no consider the formation of cyclic dimers. The new model is applied to mixtures of carboxylic acids with nonassociating compounds, and a very good description of the vapor−liquid equilibria in mixtures of alkanes + carboxylic acids is obtained.
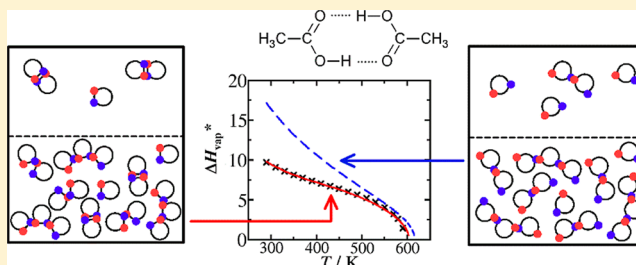
1. INTRODUCTION

Carboxylic acids represent an important class of organic compounds and are encountered in many areas of the chemical industry. Due to their high content in biofuels such as bio-oils obtained from the pyrolysis of biomass, carboxylic acids have recently received a great deal of attention from both researchers and industry. In the case of biodiesels prepared by the transesterification of oils, carboxylic acids play a dominant role since they represent the main components of the oils. The presence of organic acids is one of the factors responsible for the corrosiveness of biofuels as well as for moisture content. The reactivity of the carboxylic group also lowers the stability of such mixtures.[1] Bio-oils are complex mixtures of water and oxygenated compounds, and represent a renewable source of many classes of chemicals (including carboxylic acids) which can be used as high value compounds and raw materials in the chemical, pharmaceutical or food industries. The extraction of oxygenated compounds from bio-oils requires a thorough study of the thermodynamic properties of these fluids.

An accurate thermodynamic description of mixtures is required to reduce the amount of experimental work and design separation and purification processes. The design of a distillation column requires a precise knowledge of the vapor−liquid equilibria and vaporization enthalpies. The modeling of the thermodynamic properties of carboxylic acids such as acetic acid is not trivial as the shortest carboxylic acids tend to form dimers in the vapor phase. As a result, the experimental vaporization enthalpies of the shortest carboxylic acids are lower than the values predicted by most thermodynamic models and molecular simulations of these acids. The deviations can be larger than 80% at low temperatures. The formation of dimers in the vapor phase affects both the pure component properties and the phase behavior of mixtures. One way to accurately represent the thermodynamic properties of mixtures containing carboxylic acids is to employ a chemical

approach to describe the formation of dimers in vapor phases.[2] However, such an approach involves more adjusted parameters, and solving the chemical equilibrium can be numerically difficult.

Over the last few decades, the development of molecular based equations of state has significantly improved the description of the thermodynamic properties of mixtures over a wide range of conditions. The statistical association fluid theory (SAFT) based on the first order thermodynamic perturbation theory of Wertheim[3−7] is able to accurately describe the phase behavior of systems containing associating components[8−12] with a minimum number of parameters. The association theory of Wertheim was adopted in various equations of state. We can also cite the application of statistical association fluid theory in combination with BACK.[13] A very popular equation of state is the "cubic plus association" (CPA)[14−16] EoS that is based on a combination of the Soave−Redlich−Kwong (SRK) equation with the associative term of SAFT. Derawi et al.[17] obtained the CPA parameters for formic, acetic, and propanoic acids and studied the behavior of their mixtures with alkanes. The CPA EoS was also employed for binary mixtures of carboxylic acids with alcohols, hydrocarbons, and water and several ternary mixtures.[18−22] Using the SAFT EoS, Huang and Radosz obtained parameters for benzoic acid and for the first ten saturated linear acids by fitting the pure component VLE data.[11] Then, they studied the ability of the equation of state to predict VLE in binary systems. In the case of carboxylic acids (mixtures of formic, acetic, and propanoic acids with hydrocarbons), larger values of binary mixing parameters were required compared to analogous mixtures of *n*-alcohols with hydrocarbons.[12] Most applications of the SAFT

equation of state dealt with mixtures that are important in the petroleum and petrochemical industries, and carboxylic acids were scarcely studied. Recently, carboxylic acids have received much more attention from researchers. Lymperiadis et al.[23] obtained group parameters for carboxylic acids within the SAFT-γ approach; dos Ramos et al.[24] used a similar approach within the GC-SAFT-VR approach. Lee and Kim[25] also obtained parameters for carboxylic acids up to heptanoic acid. Piazza and Span[26] suggested a multiparameter equation of state for acetic acid, which correlates a broad range of properties in wide ranges of conditions with high accuracy. This equation also contains the classical association term of the statistical association fluid theory.

In the SAFT approach, the free energy contribution due to association depends on the assigned association scheme, i.e., on the number and the types of sites on the molecules. For carboxylic acids, two schemes are usually considered. The reader is directed to an excellent review by Breil et al.[18] of the modeling studies of carboxylic acids using SAFT-like models. Huang and Radosz[11] assigned the simplest type of bonding (denoted as the 1A association model) with a single association site that can bond with a site of the same type on another molecule. This model well describes the behavior of carboxylic acids in vapor phases where a high fraction of molecules forms doubly bonded dimers in which two carboxyl groups are in centro-symmetric orientation and form a hexagonal ring. However, in the liquid phase, the acids tend to form chain-like aggregates, which cannot be covered by the 1A model. Despite this lack, the model 1A was adopted for carboxylic acids by most authors. Breil et al.[18] were able to accurately represent the thermodynamic properties (including vaporization enthalpies) of pure acetic acid and water + acetic acid mixtures using the CPA + 1A model.

The second simplest association scheme considers two different sites A and B on molecules that can form intermolecular A−B bonds, but the bonds between sites of the same type are forbidden. This model is denoted as 2B and is commonly employed to model the association of alcohols. It was also used by Gross and Sadowski[27,28] for acetic acid. Derawi et al.[17] compared both schemes using the CPA EoS, and found that the 1A model provides better results for several binary VLE systems as well as for LLE. In a recent work, dos Ramos et al.[24] considered an asymmetric association scheme with one donor site and three acceptors for carboxylic acids within a group contribution version of the SAFT-VR theory, and they found better quality compared to 2-site and 3-site models.

Sear and Jackson suggested an extension of Wertheim's theory of fluid association, to describe the behavior of systems containing molecules that can form closed loop structures in addition to open chains.[29,30] The formation of doubly bonded dimers (DBD) as it is observed in the case of carboxylic acids represents a limiting and simplest case of their approach, in which only two-member rings (i.e., cyclic dimers or DBD) are considered. In this paper, we incorporate the approach of Sear and Jackson into the PC-SAFT EoS to describe the phase behavior of the first five carboxylic acids, and we extend the theory to mixtures of carboxylic acids + nonassociating compounds. The theoretical background is briefly resumed in the next section. In the first part of the result section, we discuss the effect of the modified association scheme on the thermodynamic properties of pure carboxylic acids; in the

second part, we analyze several binary mixtures of carboxylic acids with nonassociating compounds.

2. THEORY

The main feature of the current approach is the expression for the association contribution (A^{assoc}) to the Helmholtz free energy (see eqs 2 and 6 of ref 30, or for the special case of doubly bonded dimers, eq 1 of ref 29). In homogeneous systems, the free energy contribution due to association can be written in the following form:

$$\frac{A^{assoc}}{Vk_BT} = \sigma_\Gamma \ln \frac{\sigma_0}{\sigma_\Gamma} + \sigma_\Gamma - \sigma_A - \sigma_B + \frac{\sigma_A\sigma_B}{\sigma_0} - \sigma_A\sigma_B\Delta_{AB}$$
$$- \frac{1}{2}\sigma_0\sigma_0\Phi_{AB/BA} \tag{1}$$

This relation is an extension of the free energy association contribution for the 2B model that considers two different association sites on a molecule: for the 2B model, bonding between different sites is allowed, whereas bonding between sites of same type is prevented. In the new association scheme, the formation of cyclic dimers is allowed, which is covered by the last term of eq 1. The quantities σ in eq 1 correspond to number densities of different species considered at the equilibrium state, in agreement with Wertheim's formalism, and should not be confused with the segment diameters which are used in the next section: σ_0 is the number density of molecules with both A and B association sites nonbonded (i.e., σ_0 is the number density of "free monomers"), σ_A is the number density of molecules with nonbonded site A, i.e., the sum of molecules that are "bonded on site B/non-bonded on A", and of the "free monomers" (σ_B is defined in analogous way) and σ_Γ corresponds to the total number density of the associating molecules. The parameter Δ_{AB} corresponds to the association strength describing the formation of linear chains, and can be expressed as an integral of the product of the association Mayer function $f_{AB}(12)$ and the radial distribution function $g(12)$ of the non associated reference fluid. Within the classical SAFT approach, it is assumed that the radial distribution function is constant over the bonding volume. The integral Δ_{AB} is approximated as a product of the average value of the Mayer function, the contact value of radial distribution function in the reference system ($g_{ii}(d_{ii})$), and the bonding volume κ_{AB}

$$\Delta_{AB} = \int f_{AB}(12)g(12) \, d(12) \approx \sigma_{ii}^3\kappa_{AB}\left[\exp\left(\frac{\varepsilon_{AB}}{k_BT}\right) - 1\right]g_{ii}(d_{ii}) \tag{2}$$

The association strength ε_{AB} and the bonding volume κ_{AB} are the two parameters which describe the association. Here, we use the temperature independent diameter σ_{ii} in eq 2, as in the original version of Gross and Sadowski.[28,31] Note that some other versions of SAFT use the temperature dependent diameter d_{ii} instead of σ_{ii} in eq 2. For the contact value of the radial distribution function g_{ii}, we use the relations for hard sphere mixtures that are consistent with the BMCSL EoS.[32,33]

The second integral $\Phi_{AB/BA}$ that takes the formation of cyclic dimers into account is expressed and approximated in an analogous way

$$\Phi_{AB/BA} = \int\int f_{AB}(12)f_{BA}(12)g(12) \, d(12)$$
$$\approx \Delta_{AB}\left[\exp\left(\frac{\varepsilon_{AB}}{k_BT}\right) - 1\right]f_v \tag{3}$$

The f_v parameter in eq 3 characterizes the ability to form cyclic dimers: the product κf_v corresponds to the volume where both pairs of sites overlap.[29] If the term $\Phi_{AB/BA}$ is neglected (i.e., if $f_v = 0$), the classical 2B model is recovered.

For systems containing only one associating component, one can show that $\sigma_A = \sigma_B$, so there are only two independent densities in eq 1, which characterize the system at equilibrium: the density of free molecules, σ_0, and the density of molecules with nonbonded site A, σ_A.

Table 1. Parameters for the PC-SAFT + 1A Model

compounds	m	σ [Å]	ε/k_B [K]	κ_{AB}	ε_{AB}/k_B [K]	QAD[a] P_{sat}	QAD[a] ρ_{liq}	T range [K]
formic acid	2.1486	2.8446	249.8	5.503	2183.9	0.50	0.14	285−500
acetic acid	2.7556	2.9961	230.7	0.3663	3047.3	2.62	1.94	290−590
propionic acid	3.0940	3.1541	225.7	0.04779	4097.2	0.66	1.78	290−600
butyric acid	3.4325	3.3652	260.1	0.007202	3750.1	2.13	4.71	280−615
valeric acid	3.7710	3.4572	267.9	0.004697	3732.0	1.21	2.99	290−635

[a]Quadratic average deviation: $\text{QAD} = 100[^1/_N \sum_i\{(X_i^{cal} - X_i^{exp})/X_i^{exp}\}^2]^{1/2}$.

The equilibrium conditions are obtained by minimization of the association Helmholtz energy (eq 1) with respect to σ_A and σ_0

$$-1 + \frac{\sigma_A}{\sigma_0} = \sigma_A \Delta_{AB} \tag{4}$$

$$\frac{\sigma_\Gamma}{\sigma_0} - \frac{\sigma_A^2}{\sigma_0^2} = \sigma_0 \Phi_{AB/BA} \tag{5}$$

These equations can be reformulated using the fraction of molecules with both sites nonbonded (i.e., free monomers), $X_0 = \sigma_0/\sigma_\Gamma$, and the fraction of molecules nonbonded at site A, $X_G = \sigma_A/\sigma_\Gamma$, instead of their number densities σ_0 and σ_A.

$$-1 + \frac{X_G}{X_0} = X_G \rho_i \Delta_{AB} \tag{6}$$

$$\frac{1}{X_0} - \frac{X_G^2}{X_0^2} = X_0 \rho_i \Phi_{AB/BA} \tag{7}$$

We use the symbol X_G for this quantity in order to be consistent with the notation of Sear and Jackson;[29] nevertheless, it corresponds to X_A used in the classical TPT1 approach. The density ρ_i is the number density of the associating component, so we have $\rho_i = \sigma_\Gamma = x_i\rho$ in the case of mixtures. Equations 4 and 5 can be inserted into eq 1, and the expression for the association free energy can be rewritten in terms of X_0 and X_G as

$$\frac{A^{assoc}}{Nk_BT} = x_1\left(\ln X_0 - X_G + \frac{1}{2} + \frac{X_G^2}{2X_0}\right) \tag{8}$$

The values of X_0 and X_G are obtained as solutions of eqs 6 and 7. As it was shown by Sear and Jackson, the model is equivalent to the classical 2B model in the limiting case $f_\nu = 0$. Note that the case $f_\nu = 1$ does not correspond to the 1A model.

One major advantage of the Sear and Jackson theory compared to the classical chemical approach of dimer formation in carboxylic acid systems is the fact that only one additional parameter (f_ν) is introduced. In the chemical approach, many more parameters must be introduced to describe the temperature dependence of the equilibrium constant and the properties of dimers, which are considered as a new molecular species. Moreover, solving a chemical equilibrium in strongly non ideal systems can be numerically problematic, while solving eqs 6 and 7 is very simple with a self-substitution procedure.

In this work, we employed the new association scheme in connection with the original version of PC-SAFT EoS,[27,28] in which all the attractive contributions of the free energy except the association term are involved into the dispersion term, i.e., the dipolar, quadrupolar or polarization contributions are not considered in an explicit way. The free energy is given as a sum of different contributions,

$$\frac{A}{Nk_BT} = \frac{A^{ideal}}{Nk_BT} + \frac{A^{hc}}{Nk_BT} + \frac{A^{disp}}{Nk_BT} + \frac{A^{assoc}}{Nk_BT} \tag{9}$$

where the association term is by eq 8 for the DBD association scheme. The nonassociating part of the PC-SAFT model requires three parameters for any pure compound: the number of segments m, the segment diameter σ, and the dispersion energy ε. The reader is directed to the original paper of Gross and Sadowski[27] for the detailed description of the free energy terms (A^{ideal}, A^{hc}, and A^{disp}). Note that the Sear and Jackson theory for DBD could be easily employed within other versions of SAFT such as SAFT-VR,[34] soft-SAFT,[35] and SAFT-γ,[23,36] as well as with the CPA EoS.[14]

We have compared the results obtained with the new DBD association scheme (2B model with allowed doubly bonded dimers) with those obtained by employing the classical 2B and 1A association schemes without considering the formation of DBD. For 1A and 2B association schemes, the association contribution to the Helmholtz energy is given by

$$\frac{A^{assoc}}{Nk_BT} = x_1 \sum_a \left(\ln X_a - \frac{X_a}{2} + \frac{1}{2}\right) \tag{10}$$

where x_1 is the molar fraction of the associating component and the fractions of nonoccupied association sites X_a are obtained by solving a set of equations

$$X_a = (1 + \rho x_1 \sum_b \Delta_{ab}X_b)^{-1} \tag{11}$$

The summations in both equations run over the association sites of component 1 (in this work, we are concerned with pure carboxylic acids and mixtures with hydrocarbons), i.e., a, b = A for 1A model and a, b = A, B for 2B. The association strength Δ_{ab} is approximated by eq 2. Note that the fraction of nonbonded sites is the same for both models if the association strength Δ_{ab} has the same value. However, the association free energy is twice higher in the case of 2B model.

3. RESULTS

3.1. Parameterization. The pure component parameters (σ, ε, ε_{AB}, and κ_{AB}) for the 1A and 2B models of formic, acetic, propionic, butyric, and valeric acids were obtained by simultaneously adjusting the experimental vapor pressures and saturated liquid densities. The optimization was performed by minimizing the sum of quadratic relative deviations. The experimental vapor pressures and saturated liquid densities were actually recalculated from correlations[37] (Component Plus based on DIPPR) with a temperature increment of 5 K (about 50 points have been considered for each pure compound, between the triple and the critical points). We have checked that these correlations were close to real experimental data.[38] The aim of this study is not to find the best set of parameters for pure carboxylic acids but only to show that the improved association scheme based on the formation of DBD can lead to a significant improvement in the modeling of phase equilibria. Thus, we did not incorporate a dipolar term in the PC-SAFT model and preferred to use the original version.

The number of segments m was fixed to a prechosen value in order to lower the scatter of optimized values, which is due to the relatively flat hypersurface of the objective function. Moreover, a linear dependence of the number of segments with respect to chain length is usually observed in other homological series of compounds when PC-SAFT is used, like in the cases of n-alkanes (a = 0.3559, R^2 = 0.9991, up to C$_{20}$), 2-methylalkanes (a = 0.3362, R^2 = 0.9908, for isobutane up to

Table 2. Parameters for the PC-SAFT + 2B Model

compounds	m	σ [Å]	ε/k_B [K]	κ_{AB}	ε_{AB}/k_B [K]	QAD P_{sat}	QAD ρ_{liq}
formic acid	2.1486	2.8284	191.5	0.9962	2037.8	0.27	0.13
acetic acid	2.7556	2.9777	186.3	0.4286	2336.7	1.72	2.08
propionic acid	3.0940	3.1561	191.8	0.1585	2782.3	1.13	1.94
butyric acid	3.4325	3.3489	224.1	0.07031	2723.3	3.04	3.99
valeric acid	3.7710	3.4686	249.7	0.05080	2451.6	0.96	3.22

Table 3. Parameters for the PC-SAFT + DBD Model

compounds	m	σ [Å]	ε/k_B [K]	κ_{AB}	ε_{AB}/k_B [K]	f_v	QAD P_{sat}	QAD ρ_{liq}	QAD ρ_{vsp}
formic acid	2.1486	2.8175	186.6	0.5698	2565.2	0.02098	3.08	0.17	3.63
acetic acid	2.7556	2.9475	180.6	0.1470	3168.4	0.008815	1.14	3.06	4.1
propionic acid	3.0940	3.1333	189.3	0.1319	3075.1	0.009229	3.42	2.02	4.44
butyric acid	3.4325	3.2633	196.8	0.04082	3601.9	0.004176	5.4	4.15	3.64
valeric acid	3.7710	3.3533	209.5	0.07559	3207.0	0.01419	3.21	2.82	5.22

isoheptane), or 1-alkanols (a = 0.3300, R^2 = 0.9234, methanol–nonanol). We examined three series with different values for the acetic acid: (i) m = 1.6069 (ethane), (ii) m = 2.3827 (ethanol value), and (iii) m = 2.775 (isobutane). In the all three cases, the value for formic acid was taken to be 0.6069 smaller than the acetic acid value, since similar deviation is also observed between the first and second member in the model series (i.e., between the pairs methane–ethane, methanol–ethanol, or propane–isobutane). The series based on 2-methylalkanes provided the lowest cumulative quadratic deviation for both schemes, 1A and 2B. We employed the same values of m for the DBD approach of Sear and Jackson.

The pure component parameters for the 1A models are reported in Table 1 (together with the temperature ranges used for the optimization); those for the 2B association scheme are given in Table 2. One can observe increasing values of the ε parameter with chain length, showing an increasing role of dispersion interactions for longer acids. Although the association volume κ_{AB} monotonically decreases, the strength of association ε_{AB} approaches its maximal value between propanoic and butyric acids. The value of κ_{AB} for formic acid is rather large, which may reflect that the second H atom of this compound may also be involved in hydrogen bonding, so the 1A model is not adequate for this compound.

In the case of PC-SAFT + DBD association scheme, the optimization procedure was performed in two steps. First, we fixed the number of segments and optimized 5 parameters (σ, ε, ε_{AB}, κ_{AB}, and f_v) on vapor pressures and saturated liquid density values. As the staring values for these parameters, we took the optimized values of σ, ε, ε_{AB}, and κ_{AB} for the 2B models and used f_v = 0.001. In the case of acetic, propanoic and butyric acid, we observed, that the temperature dependence of vaporization enthalpy was also quite well reproduced, despite the optimization was performed only on P_{sat} and ρ_{liq} data, which was not reached in any of the two models within the classical approach. In a second step, we included the values of vapor coexistence densities into the objective function and reoptimised the five parameters. The overall deviations in saturated pressure and liquid density were slightly increased due to the incorporation of more data, but remained satisfactory. Note that coexistence vapor densities were calculated from the DIPPR correlations for vaporization enthalpy and vapor pressures[37] using the Clausius–Clapeyron relation. We preferred to use this property instead of the vaporization enthalpy because the vapor phase densities (or

compressibility factor Z) directly characterizes the formation of strong dimers in the vapor phase as shown by Miyamoto et al.,[2] whereas the enthalpy of vaporization includes different effects (internal energy, temperature dependence of vapor pressures, and vapor and liquid densities).

The inclusion of vapor density data into the fitting procedure for the 1A and 2B models did not significantly improve the description of vaporization enthalpies: for the 2B model of acetic acid, the mean deviations were increased to 10.6% for the vapor pressures and to 6.0% for the liquid densities, while the average deviation for the vapor phase densities was of 17.0%. Note that the association energies ε_{AB} obtained after optimization for the 1A models are significantly lower that values obtained by other authors.[18,39–41] Breil et al.[18] managed to accurately describe the vaporization enthalpy of acetic acid with the 1A model and the CPA equation of state. We have tried to fix the association energy parameter of the 1A model to a large value and optimized the other PC-SAFT parameters. We were able to get much lower values of the enthalpy of vaporization at low temperatures, but ΔH_{vap} was underestimated at high temperatures, and the overall deviations were still not satisfactory.

The parameters for PC-SAFT + DBD association scheme are reported in Table 3. The nonassociation parameters σ and ε have the same trends as for the classical association term. Also the maximal value of ε_{AB} for butyric acid is in accordance with the results obtained with the classical term; for the same acid, the association volume κ_{AB} and the factor f_v reach a minimum. We are not able to distinguish at this point whether butyric acid is an exception due to the sensitivity with respect to the experimental points or whether this effect can be interpreted at the molecular level.

The different models are compared in Figure 1 for the description of the saturated liquid densities of acetic acid, and in Figure 2 for the compressibility factor of the corresponding coexistent vapor phase (which is chosen instead of the vapor densities because of narrower range of values). The predicted vaporization enthalpies of acetic acids as function of temperature are depicted in Figure 3. The PC-SAFT + DBD can accurately describe all of the properties, liquid densities (Figure 1), vapor phase compressibility factor (Figure 2), vaporization enthalpies (Figures 3 and 4a), and vapor pressures (Figure 4b), whereas the PC-SAFT + classical 1A or 2B association schemes largely overestimate the vapor phase compressibility factors (Figure 2) and vaporization enthalpies (Figure 3), although
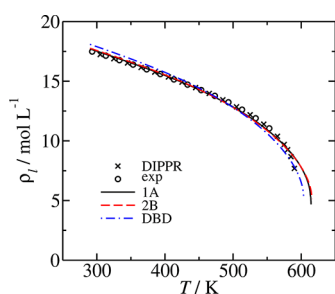
Figure 1. Liquid coexistence density of acetic acid calculated with different association models. The circles denote the experimental data (ref 38), and crosses denote the values calculated with the DIPPR correlation.[37] The different lines correspond to different association schemes.
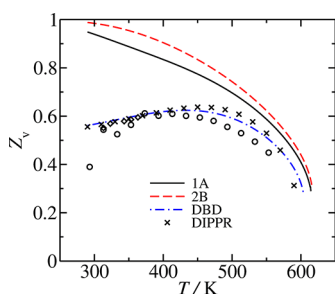

Figure 2. Compressibility factor of the coexistent vapor phase for acetic acid. The lines and symbols have the same meaning as in Figure (1). The diamonds denote the experimental data of Miyamoto et al. (ref 2). The circles denote the experimental data taken from Timmermans' book (ref 38).
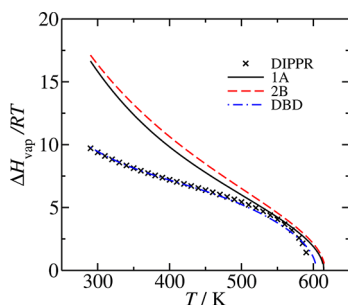
Figure 3. Vaporization enthalpy of pure acetic acid. The crosses denote values calculated with the DIPPR correlation of experimental data (ref 37), and the lines correspond to different association models (1A, 2B, and DDB schemes).

they can accurately describe liquid densities and vapor pressures. This result can be explained with the Clausius–Clapeyron expression given by

$$\Delta H_{vap} = T(v_{gas} - v_{liq})\frac{dP}{dT} \tag{12}$$

Both models 1A and 2B give a very good description of the slope dP/dT and of the saturated liquid molar volumes v_{liq}. Since these models largely overestimate v_{gas} which dominates v_{liq}, they also largely overestimate ΔH_{vap} according to eq 12. Note that the error can be as large as 80% at low temperatures for the 2B model of acetic acid. For the other carboxylic acids the observations are qualitatively the same as for acetic acid.

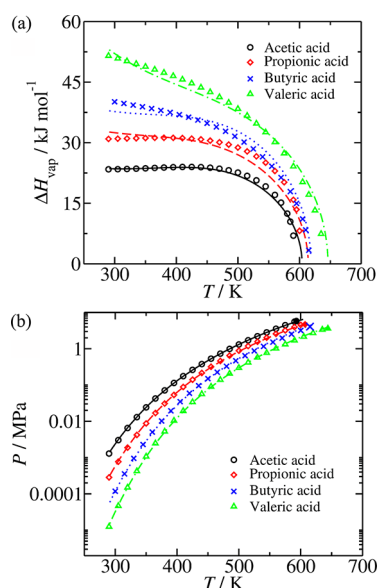The fraction of nonbonded molecules (i.e., of free monomers) in both coexistence phases is shown for acetic

Figure 4. Vapor−liquid coexistence properties of pure carboxylic acids. (a) Vaporization enthalpies and (b) vapor pressures. The symbols denote values calculated with DIPPR correlations of experimental data (ref 37), and the lines are calculated with PC-SAFT + the DBD association scheme.

acid and valeric acid in Figure 5. For the 1A model, the fraction X_A of molecules nonbonded at site A, which is defined in eq 11,
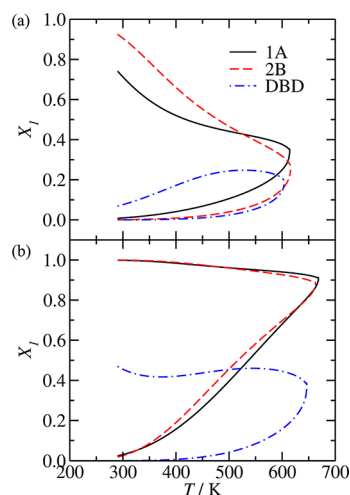

Figure 5. Fractions of nonbonded molecules along the VLE curve, for pure acetic acid (a) and pure valeric acid (b), calculated by using different association schemes: 1A (solid black line), 2B association scheme (red dashed line), and 2B + doubly bonded dimers (blue dash-dotted line). In all cases, the upper branch of the curves corresponds to the vapor phase.

corresponds exactly to the fraction of free molecules, X_1. For the PC-SAFT + 2B model the fraction of free molecules X_1 is equal to the square of the fraction of molecules with nonbonded site A, $X_1 = X_A^2$. In the new DBD approach, the fraction of molecules nonbonded at sites A and B, X_0, represents directly the fraction of molecules in monomer state ($X_0 = X_1$). One can observe in Figure 5a that the shapes of the curves for 1A and 2B models are qualitatively similar: X_1 decreases as the temperature is increased for the vapor phase, whereas X_1 increases for the liquid phase. These trends can be

explained by the functional form for the association strength: the dominant factor in the set of equations for X_A is the coexistence density.

On the other hand, the PC-SAFT + DBD model gives rise to a much lower fraction of free monomers in both phases, and both curves have closed-like shapes. Contrary to the 1A and 2B model, X_1 in the vapor phase decreases as temperature is decreased. This can be explained by a higher formation of DBD at lower temperatures. The lower tendency of valeric acid to form hydrogen bonds (Figure 5b) in both phases (compared to acetic acid) is a direct consequence of a lower value for the association volume κ_{AB}.

The fractions of molecules in different bonding states, calculated with the new DBD approach, are compared for acetic and valeric acids in Figure 6. The fraction of free molecules is
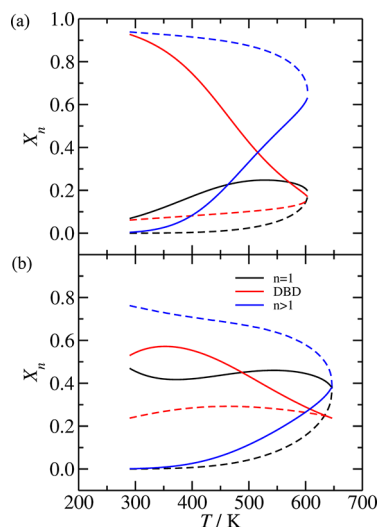

Figure 6. Fractions of nonbonded molecules (black lines), of molecules bonded as cyclic dimers (red lines), and of molecules bonded in chain-like structures (blue line) for acetic acid (a) and valeric acid (b). The dashed branches correspond to the coexistent vapor phase.

shown as the black curve, the fraction of molecules bonded in doubly bonded dimers as red; the fractions of molecules which are part of chain-like structures (including "normal" dimers) are represented by blue curves. The fraction of doubly bonded dimers can be calculated as

$$X_{dd} = 1 - \frac{X_G^2}{X_0} \tag{13}$$

Expectably, the part of molecules in nonbonded state is higher in the vapor phase, as well as the fraction of molecules bonded in cyclic dimers. However, the chain-like aggregates dominate in the liquid phase. For valeric acid the fraction of doubly bonded dimers in the liquid phase is clearly higher compared to acetic acid, whereas in the vapor phase the situation is opposite. This observation is in agreement with the values of the pure component parameters, but it can be also interpreted reasonably at the molecular scale. In the case of valeric acid, the larger nonpolar part of the molecule lowers the effective "cross section" for the formation of hydrogen bonds.

3.2. Binary Systems. In order to evaluate the quality of the different association schemes, we compared the PC-SAFT results with experimental VLE data for several binary mixtures

of carboxylic acids and n-alkanes. In all presented cases, we employed the mixing and combining rules given in Appendix A of ref.[27] Only one binary mixing parameter k_{ij} is considered and is defined as $\varepsilon_{ij} = (\varepsilon_i \varepsilon_j)^{1/2}(1 - k_{ij})$. The pure component parameters for carboxylic acids are reported in Tables 1−3. The parameters for the n-alkanes (hexane, heptane and octane) are taken from Table 2 of ref 27.

The $P-x-y$ diagrams of the n-octane + acetic acid mixture at $T = 323.15$ and 343.15 K are shown in Figures 7 and 8,
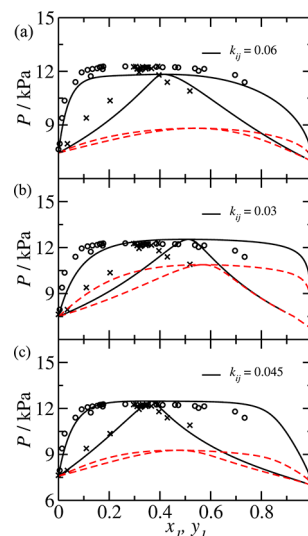

Figure 7. Vapor−liquid equilibria of the n-octane + acetic acid binary mixture at $T = 323.15$ K (equilibrium pressures as a function of octane mole fractions in both phases). The circles and crosses denote the experimental data (ref 42) and the lines are calculated with different association models and different values of the binary parameter k_{ij}: (a) 1A model with $k_{ij} = 0$ (dashed red line) and $k_{ij} = 0.06$ (solid line). (b) 2B model ($k_{ij} = 0/k_{ij} = 0.03$). (c) DBD model ($k_{ij} = 0/k_{ij} = 0.045$).
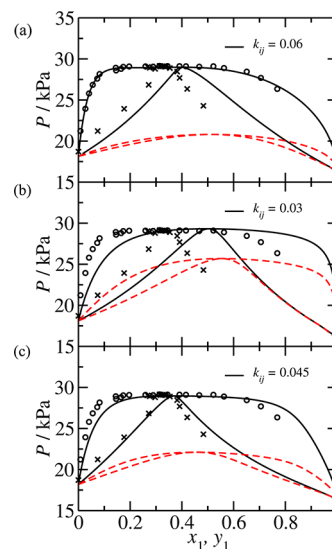

Figure 8. Vapor−liquid equilibria of the n-octane + acetic acid binary mixture at $T = 343.15$ K. The circles and crosses denote the experimental data (ref 42) and the lines are calculated with different association models and different values of the binary parameter. (a) 1A model with $k_{ij} = 0$ (dashed red line) and $k_{ij} = 0.06$ (solid line). (b) 2B model ($k_{ij} = 0/k_{ij} = 0.03$). (c) DBD model ($k_{ij} = 0/k_{ij} = 0.045$).

respectively. The different panels correspond to different association schemes: PC-SAFT-1A (a), PC-SAFT-2B (b), and PC-SAFT-DBD (c). The points are the experimental data of Plesnar et al.[42] The prediction of an azeotropic behavior is expected for this mixture, even with $k_{ij} = 0$, as the experimental vapor pressures of the pure components are rather close. All the three models predict positive azeotropes (dashed lines), but none of them is able to quantitatively predict either the maximal pressure or the composition with $k_{ij} = 0$. The solid lines in Figures 7 and 8 were obtained with values of binary mixing parameter fitted to azeotropic pressure at the highest temperature ($k_{ij} = 0.06$ for PC-SAFT-1A, 0.03 for 2B, and 0.045 for the DBD approach). After employing a binary parameter k_{ij}, the PC-SAFT-1A and PC-SAFT-DBD describe the azeotropic composition significantly better compared to the 2B model. Positive values for k_{ij} are expected for binary mixtures of polar and nonpolar compounds and this is the case here. Indeed, when a nonpolar equation of state is used, the dispersion energy parameter of the polar compound tends to describe both the dispersion interactions and some part of the dipole−dipole interactions, even if an association contribution is used.[43] Thus, the cross energy of dispersion between the non polar and the polar compound obtained from the Berthelot rule is usually overestimated,[43] and a positive k_{ij} is required to accurately describe the phase equilibria of the mixture. It may be possible to have good predictions with $k_{ij} = 0$ by using a polar version of PC-SAFT.

The 1A model describes the boiling point curve very well over the whole composition range. For the DBD model the pressures are slightly underestimated, but the dew point curve is more accurately described (Figures 7 and 8).

The $P−x−y$ diagram at $T = 313.2$ K of the n-hexane + acetic acid binary mixture is depicted in Figure 9. The values of binary mixing parameters have now values $k_{ij} = 0.05$, 0.02, and 0.035. Although in the previous case the quality of 1A model was roughly the same as of the doubly bonded dimers model, now
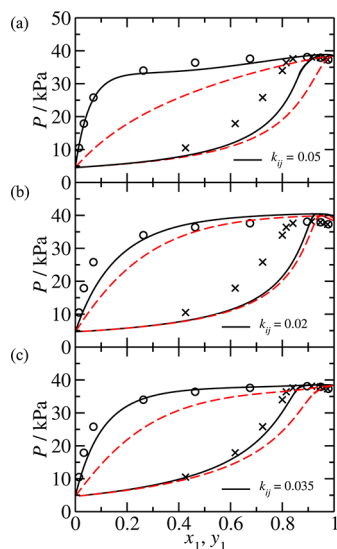
the situation is different. For the 1A model the introduction of $k_{ij} = 0.05$ leads to the prediction of the azeotropic point at $x \approx 0.95$, and the bubble point curve is well described (Figure 9a). However, the dew point curve is poorly represented. Similarly as in the 1A case, the 2B model overestimates the hexane content in both coexisting phases for a given pressure (Figure 9b). The introduction of a binary parameter can shift the bubble curve closer to the experimental values, but the dew point curve remains almost unaffected. The DBD approach with $k_{ij} = 0.035$ accurately describes both the dew and bubble point curves (Figure 9c).

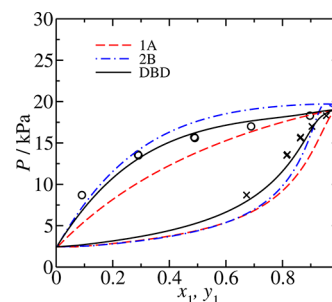The phase diagram of the n-heptane + propanoic acid mixture at $T = 313.2$ K is depicted in Figure 10. The

Figure 10. Vapor−liquid equilibria of the n-heptane + propanoic acid binary mixture at $T = 313.2$ K. The circles and crosses denote the experimental data (ref 44), and the lines are calculated with different association models with $k_{ij} = 0$.

experimental data are as in previous case by Miyamoto et al.[44] For all three approaches, the curves are calculated with $k_{ij} = 0$. Both classical approaches overestimate the content of n-heptane in the vapor phase, and both fail to describe the bubble point curve. By employing a negative value for k_{ij}, it would be possible to remove the unrealistic azeotropic point predicted by the 2B model. However, the predictions of the dew point curve would be even worse. The only satisfactory approach is the DBD model, as it can accurately predict the whole phase diagram.

For the last studied binary system (heptane + valeric acid), all approaches perform well without any binary parameter. Since we use a nonpolar version of PC-SAFT, the ε dispersion parameter for valeric acid captures a significant part of the electrostatic interactions, and these interactions are lower for valeric acid than for acetic acid. The strength of dipole−dipole interactions compared to dispersion interactions is smaller for valeric acid than for acetic acid, since valeric acid is a longer molecule. Thus, the Berthelot combining rule is more adequate for the cross interaction parameter ε_{ij}. Both the 1A and DBD models accurately represent the dew and bubble point curves well (Figure 11). The higher tendency of valeric acid to form doubly bonded dimers mentioned above leads to very close agreement between these two approaches. The 2B model overestimates the pressure along the bubble point curve.

4. CONCLUSION

The Sear and Jackson theory of doubly bonded dimers is applied with the PC-SAFT equation of state to describe the thermodynamic properties and the phase equilibria of carboxylic acids and their mixtures with hydrocarbons. It is shown that the formation of cyclic dimers in the vapor phase directly influences the compressibility factor in the vapor phase
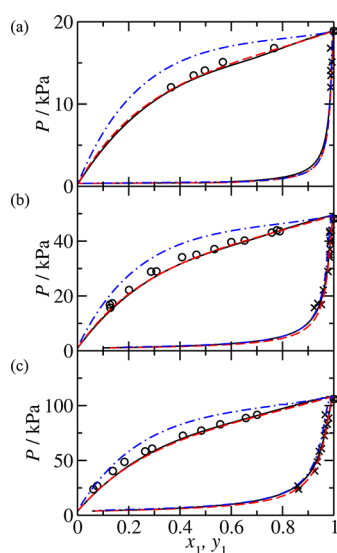

Figure 9. Vapor−liquid equilibria of the n-hexane + acetic acid binary mixture at $T = 313.15$ K. The circles and crosses denote the experimental data (ref 44) and the lines are calculated with different association models and different values of the binary parameter. (a) 1A model, $k_{ij} = 0$ (dashed red line) and $k_{ij} = 0.05$ (solid line). (b) 2B model ($k_{ij} = 0/k_{ij} = 0.02$). (c) Sear model ($k_{ij} = 0/k_{ij} = 0.035$).

Figure 11. Vapor−liquid equilibria of the *n*-heptane + valeric acid binary mixture at *T* = 323.15 (a), 348.15 (b), and 373.15 K (c). The circles and crosses denote the experimental data,[45] the lines are calculated with different association models (same symbols as in Figure 10). Here, k_{ij} = 0 for all models.

and the enthalpy of vaporization of pure carboxylic acids at low temperatures. Although the classical association models (1A and 2B) largely overestimate these properties by a factor of about 2 at low temperatures, an excellent description of the experimental data is obtained when the formation of cyclic dimers is taken into account. We extended the theory to binary mixtures of a carboxylic acid + a non-associating compound. A clear improvement of the coexistent curves in mixtures is obtained. In particular, the composition of the coexistent vapor phases is better described. The new association term that takes the formation of DBD into account can be implemented in any equation of state using the Wertheim TPT1 association theory. We intend to extend the theory to mixtures of carboxylic acids with other associating compounds such as alcohols or other acids in the near future.

■ AUTHOR INFORMATION

Corresponding Author
*Tel.:+33(0)145523531. Fax:+33(0)145528322. E-mail: patrice.paricaud@ensta-paristech.fr.

Notes
The authors declare no competing financial interest.

■ ACKNOWLEDGMENTS

■ REFERENCES

(1) Huber, G. W.; Iborra, S.; Corma, A. *Chem. Rev.* **2006**, *106*, 4044−4098.
(2) Miyamoto, S.; Nakamura, S.; Iwai, Y.; Arai, Y. *J. Chem. Eng. Data* **1999**, *44*, 48−51.
(3) Wertheim, M. S. *J. Stat. Phys.* **1984**, *35*, 19−34.
(4) Wertheim, M. S. *J. Stat. Phys.* **1984**, *35*, 35−47.
(5) Wertheim, M. S. *J. Chem. Phys.* **1986**, *85*, 2929−2936.
(6) Wertheim, M. S. *J. Stat. Phys.* **1986**, *42*, 459−476.
(7) Wertheim, M. S. *J. Chem. Phys.* **1987**, *87*, 7323−7331.
(8) Chapman, W. G.; Gubbins, K. E.; Jackson, G.; Radosz, M. *Fluid Phase Equilib.* **1989**, *52*, 31−38.
(9) Chapman, W. G.; Gubbins, K. E.; Jackson, G.; Radosz, M. *Ind. Eng. Chem. Res.* **1990**, *29*, 1709−1721.
(10) Chapman, W. G.; Jackson, G.; Gubbins, K. E. *Mol. Phys.* **1988**, *65*, 1057−1079.
(11) Huang, S. H.; Radosz, M. *Ind. Eng. Chem. Res.* **1990**, *29*, 2284−2294.
(12) Huang, S. H.; Radosz, M. *Ind. Eng. Chem. Res.* **1991**, *30*, 1994−2005.
(13) Zhang, Z. Y.; Yang, J. C.; Li, Y. G. *Fluid Phase Equilib.* **2000**, *172*, 111−127.
(14) Kontogeorgis, G. M.; Voutsas, E. C.; Yakoumis, I. V.; Tassios, D. P. *Ind. Eng. Chem. Res.* **1996**, *35*, 4310−4318.
(15) Kontogeorgis, G. M.; Michelsen, M. L.; Folas, G. K.; Derawi, S.; vonSolms, N.; Stenby, E. H. *Ind. Eng. Chem. Res.* **2006**, *45*, 4855−4868.
(16) Kontogeorgis, G. M.; Michelsen, M. L.; Folas, G. K.; Derawi, S.; vonSolms, N. *Ind. Eng. Chem. Res.* **2006**, *45*, 4869−4878.
(17) Derawi, S. O.; Zeuthen, J.; Michelsen, M. L.; Stenby, E. H.; Kontogeorgis, G. M. *Fluid Phase Equilib.* **2004**, *225*, 107−113.
(18) Breil, M. P.; Kontogeorgis, G. M.; Behrens, P. K.; Michelsen, M. L. *Ind. Eng. Chem. Res.* **2011**, *50*, 5795−5805.
(19) Folas, G. L.; Derawi, S. O.; Michelsen, M. L.; Stenby, E. H.; Kontogeorgis, G. M. *Fluid Phase Equilib.* **2005**, *228*, 121−126.
(20) Oliveira, M. B.; Queimada, A. J.; Kontogeorgis, G. M.; Coutinho, J. A. P. *J. Supercrit. Fluids* **2009**, *55*, 876−892.
(21) Perakis, C. A.; Voutsas, E. C.; Magoulas, K. G.; Tassios, D. P. *Ind. Eng. Chem. Res.* **2007**, *46*, 932−938.
(22) Kontogeorgis, G. M.; Folas, G. K.; Muro-Sune, N.; vonSolms, N.; Michelsen, M. L.; Stenby, E. H. *Fluid Phase Equilib.* **2007**, *26*, 205−211.
(23) Lymperiadis, A.; Adjiman, C. S.; Jackson, G.; Galindo, A. *Fluid Phase Equilib.* **2008**, *274*, 85−104.
(24) dosRamos, M. C.; Haley, J. D.; Westwood, J. R.; McCabe, C. *Fluid Phase Equilib.* **2011**, *306*, 97−111.
(25) Lee, B. S.; Kim, K. C. *Korean J. Chem. Eng.* **2007**, *24*, 133−147.
(26) Piazza, L.; Span, R. *Fluid Phase Equilib.* **2011**, *303*, 134−149.
(27) Gross, J.; Sadowski, G. *Ind. Eng. Chem. Res.* **2001**, *40*, 1244−1260.
(28) Gross, J.; Sadowski, G. *Ind. Eng. Chem. Res.* **2002**, *41*, 5510−5515.
(29) Sear, R. P.; Jackson, G. *Mol. Phys.* **1994**, *82*, 1033−1048.
(30) Sear, R. P.; Jackson, G. *Phys. Rev. E* **1994**, *50*, 386−394.
(31) Gross, J.; Spuhl, O.; Tumakaka, F.; Sadowski, G. *Ind. Eng. Chem. Res.* **2003**, *42*, 1266−1274.
(32) Boublík, T. *J. Chem. Phys.* **1970**, *53*, 471−472.
(33) Mansoori, G. A.; Carnahan, N. F.; Starling, K. E.; Leland, T. W. **1971**, *54*, 1523-1525.
(34) Gil-Villegas, A.; Galindo, A.; Whitehead, P. J.; Mills, S. J.; Jackson, G. *J. Chem. Phys.* **1997**, *106*, 4168−4186.
(35) Llovell, F.; Pàmies, J. C.; Vega, L. F. *J. Chem. Phys.* **2004**, *121*, 10715−10724.
(36) Avendaño, C.; Lafitte, T.; Galindo, A.; Adjiman, C. S.; Jackson, G.; Müller, E. A. *J. Phys. Chem. B* **2011**, *115*, 11154−11169.
(37) Prosim. Component Plus database (based on DIPPR); 3.8.0.1 ed., 2001.
(38) Timmermans, J. *Physico-chemical constants of pure organic compounds*; Elsevier: Amsterdam, 1965; Vol. *II*.
(39) Kleiner, M.; Tumakaka, F.; Sadowski, G. *Thermodynamic modeling of complex systems*; Springer: Berlin, 2008
(40) Muro-Suñé, N.; Kontogeorgis, G.; von Solms, N.; Michelsen, M. L. *Ind. Eng. Chem. Res.* **2008**, *47*, 5660−5668.
(41) Soo, C.-B. Experimental thermodynamic measurements of biofue-related associating compunds and modelling using the PC-SAFT equation of state., PhD Thesis, Mines Paris Tech, 2011.

7881

dx.doi.org/10.1021/jp303051j | *J. Phys. Chem. B* 2012, 116, 7874−7882

(42) Plesnar, Z.; Fu, Y.-H.; Sandler, S. I.; Orbey, H. *J. Chem. Eng. Data* **1996**, *41*, 799−801.

(43) Haslam, A. J.; Galindo, A.; Jackson, G. *Fluid Phase Equilib.* **2008**, *266*, 105−128.

(44) Miyamoto, S.; Nakamura, S.; Iwai, Y.; Arai, Y. *J. Chem. Eng. Data* **2000**, *45*, 857−861.

(45) Lodl, S. J.; Scheller, W. A. *J. Chem. Eng. Data* **1967**, *12*, 485−488.

7882

dx.doi.org/10.1021/jp303051j | *J. Phys. Chem. B* 2012, 116, 7874−7882